PROCEEDINGS OF SCIENCE

The real-time finite-temperature static potential: a higher order calculation

Margaret E. Carrington,[a,b] **Cristina Manuel**[c,d] **and Joan Soto**[f,d,*]

[a] *Department of Physics, Brandon University, Brandon, Manitoba R7A 6A9, Canada*
[b] *Winnipeg Institute for Theoretical Physics, Winnipeg, Manitoba, Canada*
[c] *Instituto de Ciencias del Espacio (ICE, CSIC)*
C. Can Magrans s.n., 08193 Cerdanyola del Vallès, Catalonia, Spain
[d] *Institut d'Estudis Espacials de Catalunya (IEEC)*
08860 Castelldefels (Barcelona), Catalonia, Spain
[f] *Departament de Física Quàntica i Astrofísica and Institut de Ciències del Cosmos, Universitat de Barcelona, Martí i Franquès 1, 08028 Barcelona, Catalonia, Spain*

E-mail: carrington@brandonu.ca, cristina.manuel@csic.es, joan.soto@ub.edu

We report on a calculation of the real-time QCD static potential in a high temperature medium in the region where bound states transit from narrow resonances to wide ones. The calculation involves loop diagrams calculated in the Hard Thermal Loop (HTL) effective theory and power corrections to the HTL Lagrangian calculated in QCD. We compare our results with recent lattice data and check the consistency of different methods used in lattice calculations. We also discuss the usefulness of our results to guide lattice inputs.

The XVIth Quark Confinement and the Hadron Spectrum Conference (QCHSC24)
19-24 August, 2024
Cairns Convention Centre, Cairns, Queensland, Australia

*Speaker

 ISSN 1824-8039 . Published by SISSA Medialab.

PoS(QCHSC24)152

1. Introduction

The zero temperature QCD static potential is Coulomb-like at short distances and linearly rising at long distances. At finite temperature the short-distance Coulomb-like potential becomes screened which leads to the idea that heavy quark-antiquark bound state production in Heavy Ion Collision (HIC) experiments will be suppressed through screening. However it turns out that another effect is more important. The static potential develops an imaginary part that becomes larger than the real part before the screening effects become sizable. This means that bound states disappear because they become wide resonances rather than because they are no longer supported by the Yukawa-like potential [1]. The suppression of heavy quark bound state production is observed in current Heavy Ion Collision (HIC) experiments in a pattern that is consistent with this idea. We present here a calculation of the real-time QCD static potential in a high temperature medium in the regime where bound states start melting [2]. The calculation goes beyond the leading order result of ref. [1] in a controlled way and provides the first check that the above mentioned mechanism survives higher order corrections.

The static potential is defined as the ground-state energy of a static quark and a static antiquark separated at a distance r. The calculation amounts to that of the expectation value of a rectangular Wilson loop with the length of the temporal sides of the loop taken to infinity. In practice, when the coupling constant g is small, it can be carried out as a matching calculation between Non-Relativistic QCD (NRQCD) and Potential Non-Relativistic QCD (pNRQCD) by standard diagramatic techniques [3, 4]. We work in the close-time-path formalism of thermal field theory. The static quark and antiquark are (unthermalised) probe particles for which only the longitudinal photon (A_0) vertices in the time-ordered branch are relevant. We use the Coulomb gauge and dimensional regularization throughout.

The leading order (LO) result for the momentum space potential, under the assumptions that $g \ll 1$ and the typical momentum exchange between the quark-antiquark satisfies $p \ll T$, is [1]

$$V_{\rm 1lo}(p) = g^2 C_F G(0,p) \quad , \quad G(0,p) = -\frac{1}{m_D^2 + p^2} + \frac{i\pi T m_D^2}{p\left(m_D^2 + p^2\right)^2} \tag{1}$$

where $C_F = (N_c^2 - 1)/(2N_c)$, N_c is the number of colors, $m_D = gT\hat{m}_D$ is the Debye mass, with $\hat{m}_D = \sqrt{(N_c + N_f/2)/3}$, T is the temperature, N_f is the number of light flavors, and $G(p_0, p)$ the time-ordered longitudinal HTL propagator. The imaginary part arises from a subtle cancellation of the Bose enhanced symmetric term in $G(p_0, p)$, proportional to T/p_0, and contributions of the HTL selfenergy proportional to p_0 when $p_0 \to 0$.

For a narrow resonance to exist the imaginary part of the static potential must be smaller than the real part. This implies that $p > (m_D^2 T)^{1/3} \sim g^{2/3} T$ or $p = g^a T$ with $0 < a < 2/3$ (which we call a semi-hard scale). The value $a = 2/3$ gives the momentum scale for which the real and imaginary parts of the leading order momentum space potential are of the same size. Parametrically, it is the scale at which we expect quarkonium to dissociate. We arrange our calculation so that the most important corrections above this scale, namely for $a < 2/3$, are taken into account. Since the LO calculation [1] corresponds to a tree-level one-gluon exchange in HTL EFT, we expect the leading corrections to be included in the one-loop HTL calculation and in the power corrections to the HTL Lagrangian. We will take into account all corrections larger than g^2 to the real part and

larger than g^{3a} and g^{2-a} to the imaginary part of the LO momentum space potential. Note that the scaling in a at LO is different for the real (g^{2-2a}/T^2) and the imaginary parts (g^{4-5a}/T^2). Two loop diagrams give corrections of order g^2 or smaller to the real part, and of order g^{3a} or smaller to the imaginary part. Including full HTL vertices in the self-energy diagrams gives corrections of order g^2 or smaller to the real part and of order g^{2-a} or smaller to the imaginary part. All together our conditions restrict a to be in the range $1/2 < a < 2/3$[1] .

2. The static potential in momentum space

The relevant diagrams are shown in Fig. 1, where the (solid) fermion lines do not depend on the spatial momenta (the static limit) and the curly lines are HTL longitudinal gluon propagators. There is one (4-dimensional) momentum variable that is integrated over (which we call k) and the momentum transfer is $p = (p_0, \vec{p})$.

2.1 Selfenergy diagrams

Since the gluon selfenergy (in Fig. 1 (a)) has dimension 2 and the external momentum p is semi-hard, the largest contribution arises when the loop momentum k is hard ($k \sim T$). The dominant contribution in this case is already taken into account in the tree-level exchange of the HTL propagator. The leading sub-dominant contribution in the p/T expansion, the so called power correction, is also relevant to us. The next larger contribution is when k is also semi-hard. Since $k \gg m_D$, HTL vertices and HTL propagators reduce to the bare ones up to corrections of order m_D^2/p^2. In addition, since the semi-hard scale is still smaller than the hard scale T, the thermal distributions can be expanded, which leads to the Pauli blocking of the quark loops, which can then be neglected, and to Bose enhancement of the gluon ones. Infinitesimal contributions proportional to p_0 must be kept in both cases, k hard and k semi-hard, as they may cancel against factors T/p_0 from the Bose distribution. The gluon self-energy bubble in Fig. 1(a) for $p_0 \to 0$ reads,

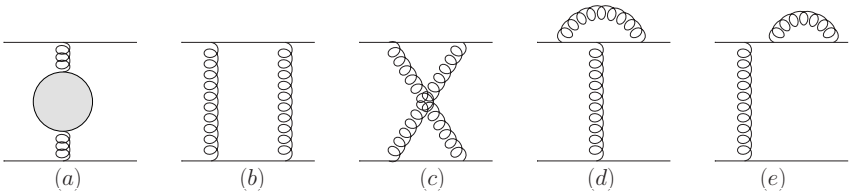

Figure 1: One-loop contributions to the static potential in the Coulomb gauge. All gluon lines correspond to HTL longitudinal gluons. The iteration of the LO potential must be subtracted from diagram (b). Note that there is no diagram analogous to (d) with a three-gluon vertex. Diagram (e) is a reminder that the wave function renormalization of the static quarks must be taken into account.

$$\Pi^{\rm ret}_{\rm nlo}(p_0, \vec{p}) = -\frac{g^2 T}{4}\left(N_c\left(p + i\,\frac{7}{3}\,\frac{p_0}{\pi}\right) - i\left(N_c - \frac{N_f}{2}\right)\frac{p_0\, p}{2\pi T}\right) . \tag{2}$$

[1] We correct a misprint in [2].

The first contribution comes from the loop with k semi-hard [5–7] and the second piece is the power correction. The self-energy Eq.(2) leads to the following contribution to the potential,

$$V_2^{(\mathrm{a})}(p) = -g^4 C_F N_c \left[\frac{p\,T}{4(p^2+m_D^2)^2} + i \left(\frac{\frac{7}{3}T^2}{2\pi(p^2+m_D^2)^2} - \frac{pT\left(1-\frac{N_f}{2N_c}\right)}{4\pi\left(p^2+m_D^2\right)^2} \right) \right] \tag{3}$$

2.2 Vertex and wave function renormalization diagrams

There is no hard contribution ($k_0 \sim T$) from diagrams (d,e) of Fig. 1 because, in the Coulomb gauge, there is no k_0 dependence in the longitudinal gluon propagator of QCD. The only possible contributions must come from the HTL Lagrangian. Since the static quarks are blind to p (static limit), k must be soft ($k \sim m_D$). Their contribution to the potential in momentum space then reads,

$$V_2^{(\mathrm{de})}(p) = i g^4 N_c C_F G(0,p) \int \frac{d^4k}{(2\pi)^4} \frac{G(k_0,k)}{(k_0+i\eta)^2}\,, \tag{4}$$

with $\eta \to 0^+$. Since $k \sim m_D \ll T$, the Bose distribution can be expanded. Then the k_0 integral can be done by contour integration, and the remaining k integral can be carried out analytically.

2.3 Ladder and cross-ladder diagrams

Diagrams (b,c) in Fig. 1 have dimension -2. Hence, the largest contribution comes from the smallest scale, $k \sim m_D$. Diagram (b) requires the subtraction of the iteration of the LO potential, which cancels the pinch singularities. The final contribution of the two diagrams reads,

$$V_2^{(\mathrm{bc})}(p) = -\frac{i g^4 N_c C_F}{2} \int \frac{d^4k}{(2\pi)^4} \frac{G(k_0,|\vec{k}+\vec{p}|)G(k_0,k)}{(k_0+i\eta)^2}\,. \tag{5}$$

Even with the Bose distributions expanded ($k_0 \sim m_D \ll T$), the integral cannot be carried out analytically for arbitrary p. Fortunately, since in our case $p \gg k, k_0$ we can write under the integral sign,

$$G(k_0,|\vec{k}+\vec{p}|) = G(0,p)\left[1 - \frac{k^2}{3} G(0,p)\left(1+4m_D^2 G(0,p)\right)\right] + O\left(\frac{m_D^3}{p^5}\right). \tag{6}$$

$G(0,p)$ could be further expanded in m_D/p. However, it is convenient to keep it in this form, since $G(0,p)$ appears at LO (1), in the self-energy contributions Eq.(3) and in the vertex contributions Eq.(4). We call it the damped approximation. Note that the leading term in Eq.(6) has the same form as Eq.(4) when we substitute it in Eq.(5). We display both contributions together,

$$\begin{aligned} V_2^{(\mathrm{de})}(p) + V_2^{(\mathrm{bc})}(p) \;=\; & \frac{1}{2} g^4 N_c C_F \left[-\frac{i\left(3\pi^2-16\right)}{128\pi} \frac{\pi T^2 m_D}{p(p^2+m_D^2)^2} \right. \\ & \left. + \frac{T}{m_D}\left(\frac{3\pi^2-16}{128\pi\left(p^2+m_D^2\right)} - \frac{m_D^2(\pi^2-16)}{384\pi\left(p^2+m_D^2\right)^2} \right) \right] \end{aligned} \tag{7}$$

3. The static potential in coordinate space

The coordinate space potential can be obtained by Fourier transforming the momentum space potential,

$$V(r) = \int \frac{d^3p}{(2\pi)^3}\, e^{i\vec{p}\cdot\vec{r}}\, V(p)\,. \tag{8}$$

The LO expression from (1) reads, $V(p) = V_{\rm 1lo}(p) = g^2 C_F G(0,p)$,

$$V_{\rm 1lo}(r) = -\frac{g^2 C_F}{4\pi\hat{r}}\left(m_D e^{-\hat{r}} - 2iT\, I_2(\hat{r})\right) \quad , \quad I_j(\hat{r}) = \int_0^\infty d\hat{p}\, \sin(\hat{p}\hat{r})\, (\hat{p}^2+1)^{-j}\,, \tag{9}$$

($\hat{r} \equiv r m_D$, $\hat{p} \equiv p/m_D$). We are interested in describing bound states before they disappear, and this happens before screening effects become important, namely when $m_D r \ll 1$. The integral (8) gets contributions from $p \sim 1/r \gg m_D$, which is the region in which we have calculated $V(p)$, and from $p \sim m_D$, a region for which the calculations are far more cumbersome, and we have not carried them out. However, in this second region, the contributions to $V(r)$, which we call $V_{\rm soft}(r)$, become universal.

3.1 The soft region

Since $r m_D \ll 1$, for $p \sim m_D$ the exponential can be expanded,

$$V_{\rm soft}(r) = \int_{p\lesssim m_D} \frac{d^3p}{(2\pi)^3}\, e^{i\vec{p}\cdot\vec{r}}\, V(p) = \int_{p\lesssim m_D} \frac{d^3p}{(2\pi)^3}\left(1 + i\vec{p}\vec{r} - \frac{1}{2}(\vec{p}\vec{r})^2 + \cdots\right) V(p, m_D)\,. \tag{10}$$

The second term is zero by symmetry in an isotropic system. The contribution from the soft momentum region thus reduces to a polynomial in r^2. At the order to which we work we need the zeroth order (the r-independent term) for the real part and up to the first order (the r^2 term) in the imaginary part [2]. The form of the soft contributions to the coordinate space potential is then

$$V_{2,\rm soft}(r) = g^4 q_0 T + i\left(g^3 i_0 T + g^5 i_2 r^2 T^3\right)\,, \tag{11}$$

where $(q_0,\, i_0,\, i_2)$ are real constants, which parametrize our ignorance on the soft region at the desired order. We can verify that Eq.(11) is the correct form for the soft contributions by expanding the NLO result in m_D/p and Fourier transforming the result. The coordinate space expression has poles of order $1/(d-3)$ that can be absorbed into the parameters of Eq.(11).

3.2 The semi-hard region

We display here the result for the Fourier transform of our calculations, $V(p) = V_2^{(\rm a)}(p) + V_2^{(\rm bc)}(p) + V_2^{(\rm de)}(p)$, in the damped approximation. The Fourier transform of the damped approximation includes part of the soft contributions. The apparent difference between the damped approximation and the fully expanded result, which only takes into account the semi-hard contribution, is compensated by the different values that (q_0, i_0, i_2) take in each case.

$$\begin{aligned}
{\rm Re}[V_2] &= \frac{g^4 N_c C_F T}{64\pi^2\hat{r}}\left\{8\,(I_2(\hat{r}) - I_1(\hat{r})) + \frac{e^{-\hat{r}}}{16}\left(3\pi^2 - 16 + \frac{\hat{r}}{6}\left(16-\pi^2\right)\right)\right\} \\
i{\rm Im}[V_2] &= -i\frac{g^3 C_F\, T}{16\pi^2 \hat{m}_D}\left\{\frac{3\pi^2-16}{32\,\hat{r}} I_2(\hat{r}) + \frac{7}{3}\, N_c e^{-\hat{r}} - \frac{2g\hat{m}_D}{\pi\hat{r}}\left(N_c - \frac{N_f}{2}\right)(I_1(\hat{r}) - I_2(\hat{r}))\right\}.
\end{aligned} \tag{12}$$

The first (second) line of the real (imaginary) part comes from Fig. 1(a) and the remaining contri-butions from the last four diagrams in Fig. 1.

4. Comparison with lattice results.

Even though our calculation holds in a very specific setting, we want to test here how it compares to lattice calculations, which have a more general set up.

First we compare our potential with [8]. We take $N_c = N_f = 3$ and fix g from the fit to the $T = 0$ lattice data for the static potential with $r \in [0, 0.3]$ fm which delivers $g = 1.8$. Note that the running of $g = g(T)$ is higher order in our counting. The constants (q_0, i_0, i_2) are determined by fitting to the lattice data at all available temperatures and values of r between 0.04 and 0.3 fm. In order to adjust the origin of energies, we also add a temperature independent constant S to the real part of the potential. The values we obtain are $(q_0, i_0, i_2) = (0.027, -0.019 \pm 0.001, 0.194 \pm 0.002)$ and $S = 219$ MeV. We also adjust the origin of energies for the LO potential and obtain $S_{\rm lo} = 200$ MeV. We show our results in Fig. (2) for $S_{\rm avg} = (S + S_{\rm lo})/2 = 209.5$ MeV. If we ignore the soft contributions ($q_0 = i_0 = i_2 = 0$), our results are still closer to data than the LO result, although the improvement is marginal. When we include them, we observe that the real part of the potential varies very little with temperature, in agreement with the data. This is non-trivial since the soft contribution is independent of r. For the imaginary part of the potential most of the contribution comes from the soft region, which produces a large correction to the LO result.

Next we compare with the results of [9]. We focus on the bottomonium ground state, since it is the heavy quarkonium state best suitable for weak coupling calculations. We take $N_c = N_f = 3$, the mass of the bottom quark $m_b = 4676$ MeV, and $g = 1.8$, as obtained in the previous comparison. We then solve the Schrödinger equation using our result for the real part of the potential in the damped approximation. We find the binding energy of the ground state at all temperatures available and subtract the Coulomb binding energy. In order to match the definition of Ref. [9], the widths for each temperature are obtained by calculating the expectation value $-\langle {\rm Im}[V]\rangle$. The constants (q_0, i_0, i_2) are determined by fitting to the lattice data at all available temperatures and their values are $(q_0, i_0, i_2) = (0.044 \pm 0.002, -0.026 \pm 0.009, 0.052 \pm 0.002)$. The results are shown in Fig. 3. If we ignore the soft contributions, we slightly improve (worsen) the description of the decay width (binding energy). When we include them, the temperature dependence of both the binding energy and the decay width gives a reasonable description of lattice data, and a considerable improvement with respect to the LO results.

We can use our results for the binding energies and widths to estimate the dissociation temperature. The dissociation temperature of a bound state can be defined as the temperature for which its thermal decay width equals the energy difference to the closest state, at which point we are not able to distinguish a given state from its neighbor in the spectral function. For simplicity, we will use instead the energy difference to the threshold, which is expected to provide a slightly higher dissociation temperature. The decay width is defined to be the expectation value of $-2{\rm Im}[V]$. The leading order result is $T_{\rm diss} = 193.2$ MeV and the damped approximation gives $T_{\rm diss} = 210$ MeV if we ignore the soft contributions, $T_{\rm diss} = (202 \pm 10)$ MeV using the fits to Ref. [9], and $T_{\rm diss} = (142.7 \pm 1.1)$ MeV using the fits to Ref. [8].

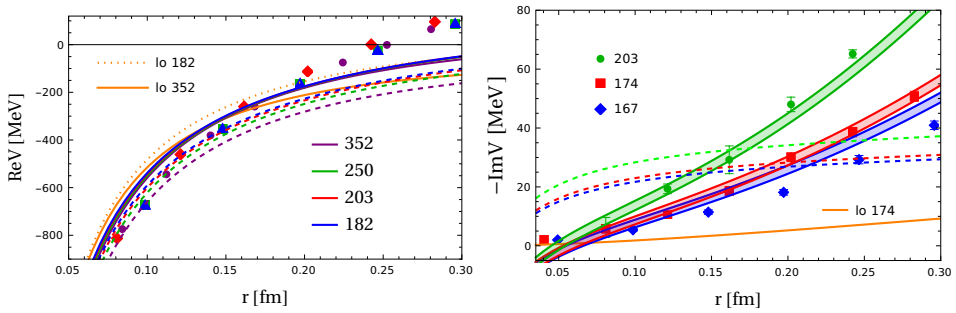

Figure 2: Real and imaginary part of V. Dashed (solid) lines correspond to $V = V_{1\text{lo}} + V_2$ ($V = V_{1\text{lo}} + V_2 + V_{2,\text{soft}}$) in the damped approximation with parameters given in the text. The legends indicate the temperature in MeV. The real part includes a global shift of $S_{\text{avg}} = 209.5$ MeV for all curves. The LO contribution (HTL) includes the one-loop static quark self-energies. For the imaginary part, we show a single temperature since the remaining two would overlap with it. The solid bands on the right plot indicate the uncertainty.

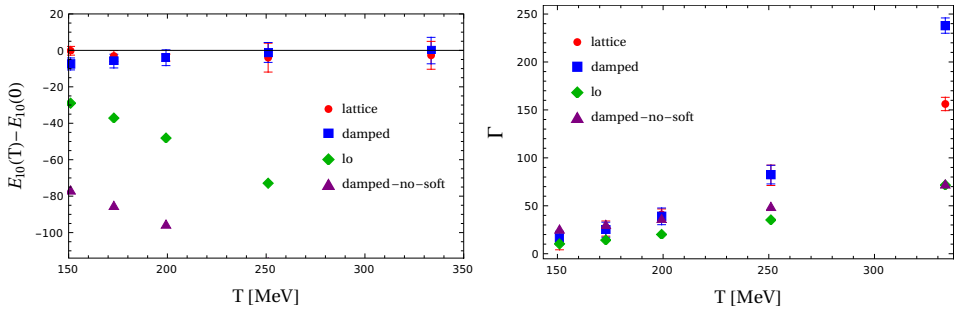

Figure 3: The temperature dependence of the binding energy and thermal width (in MeV) of the bottomonium ground state. The *lo* includes the one-loop static quark self-energies.

Our approach is able to reasonably describe the two sets of lattice data [8] and [9]. However, the parameter sets we need in order to do so are not entirely consistent. Since in our approach all scales are explicit, we expect the same size for the numerical coefficients obtained from the two fits. This is true for all coefficients in the two sets except for i_2 in the set of Ref. [8]. The outcomes for q_0 differ by only a factor ≈ 0.61, for i_0 by a factor ≈ 0.73, but for i_2 they differ by a factor ≈ 3.7. The dissociation temperature we obtain from the set of Ref. [8] is also very low.

5. Summary and conclusions.

We have calculated the momentum space potential including corrections beyond the leading order HTL result, when the typical momentum transfer p satisfies $m_D \ll p \ll T$. This is the relevant region to obtain the dissociation temperature for heavy quarkonium. We have extended our calculation to softer p by keeping suitable $p^2 + m_D^2$ terms unexpanded, which we have called the damped approximation. We also include the power corrections calculated in QCD. The coordinate space potential is then determined for $1/T \ll r \ll 1/m_D$ up to a polynomial in r^2, which encodes the contribution for $p \lesssim m_D$ at any order in g. We expect our expressions Eqs (12) and (13), with the addition of Eq.(11), to be reasonable approximations at larger r as well, since explicit damping factors are kept. Hence, we expect they will provide useful inputs for the Bayesian methods required in the

effort to determine the real-time static potential from lattice QCD. As an example, we have shown that our results describe reasonable well two different sets of lattice data, whereas the LO result fails to do so. We have also been able to identify an inconsistency between these two sets of data.

Acknowledgments. We thank Peter Petreczky and Rasmus Larsen for providing the data of Refs. [9] and [8], respectively. MEC acknowledges support by the Natural Sciences and Engineering Research Council of Canada under grant SAPIN-2023-00023 and thanks ICCUB and ICE for hospitality. CM was supported by Ministerio de Ciencia, Investigación y Universidades (Spain) MCIN/AEI/10.13039/501100011033/ FEDER, UE, under the project PID2022-139427NB-I00, by Generalitat de Catalunya by the project 2021-SGR-171 (Catalonia), and also partly supported by the Spanish program Unidad de Excelencia Maria de Maeztu CEX2020-001058-M, financed by MCIN/AEI/10.13039/501100011033. JS acknowledges financial support from Grant No. 2017-SGR-929 and 2021-SGR-249 from the Generalitat de Catalunya and from projects No. PID2022-136224NB-C21, PID2022-139427NB-I00 and No. CEX2019-000918-M from Ministerio de Ciencia, Innovación y Universidades.

References

[1] M. Laine, O. Philipsen, P. Romatschke and M. Tassler, *Real-time static potential in hot QCD*, *JHEP* **03**, 054 (2007) [hep-ph/0611300].

[2] M. E. Carrington, C. Manuel and J. Soto, *High-Temperature QCD Static Potential beyond Leading Order*, *Phys. Rev. Lett.* **134**, no.1, 011905 (2025) [arXiv:2407.00310 [hep-ph]].

[3] N. Brambilla, A. Pineda, J. Soto and A. Vairo, *Effective Field Theories for Heavy Quarkonium, Rev. Mod. Phys.* **77**, 1423 (2005) [arXiv:hep-ph/0410047 [hep-ph]].

[4] A. Pineda, *Review of Heavy Quarkonium at weak coupling*, *Prog.Part.Nucl.Phys.* **67**, 735-785 (2012) [arXiv:1111.0165 [hep-ph]].

[5] A. K. Rebhan, *The NonAbelian Debye mass at next-to-leading order*, *Phys. Rev. D* **48**, R3967 (1993) [hep-ph/9308232].

[6] C. Y. Shi, J. Q. Zhu, Z. L. Ma and Y. D. Li, *Thermal Width for Heavy Quarkonium in the Static Limit*, *Chin. Phys. Lett.* **32**, 121201, (2015).

[7] J. Q. Zhu, Z. L. Ma, C. Y. Shi and Y. D. Li, *Thermal single-gluon exchange potential for heavy quarkonium in the static limit*, *Nucl. Phys. A* **942**, 54 (2015).

[8] A. Bazavov *et al.* [HotQCD], *Unscreened forces in the quark-gluon plasma?*, *Phys. Rev. D* **109**, no.7, 074504 (2024) [arXiv:2308.16587 [hep-lat]].

[9] R. Larsen, S. Meinel, S. Mukherjee and P. Petreczky, *Excited bottomonia in quark-gluon plasma from lattice QCD*, *Phys. Lett. B* **800**, 135119 (2020) [hep-lat/1910.07374].